

## Automatic Image Quality Assessment with Application in Biometrics

H. Fronthaler, K. Kollreider and J. Bigun

Halmstad University

SE-30118, Sweden

{hartwig.fronthaler, klaus.kollreider, josef.bigun}@ide.hh.se

### Abstract

*A method using local features to assess the quality of an image, with demonstration in biometrics, is proposed. Recently, image quality awareness has been found to increase recognition rates and to support decisions in multimodal authentication systems significantly. Nevertheless, automatic quality assessment is still an open issue, especially with regard to general tasks. Indicators of perceptual quality like noise, lack of structure, blur, etc. can be retrieved from the orientation tensor of an image, but there are few studies reporting on this. Here we study the orientation tensor with a set of symmetry descriptors, which can be varied according to the application. Allowed classes of local shapes are generically provided by the user but no training or explicit reference information is required. Experimental results are given for fingerprint. Furthermore, we indicate the applicability of the proposed method to face images.*

### 1. Introduction

Automatic assessment of image quality by a machine expert is difficult, but useful for a number of tasks: monitor and adjust image quality, optimize algorithms and parameter settings, benchmark image processing systems [1]. Quality assessment methods can be divided into full/reduced/no-reference approaches, depending on how much prior information is available on how a perfect candidate image should look like. In this work we demonstrate quality assessment of the second kind, where images come from a specific application. The use of general quality metrics originally suggested in image compression studies [2], e.g. mean square error (MSE) or peak signal to noise ratio (PSNR) is excluded because of poor performance in recognition applications. Also, a “universal” quality metric appears to be impossible: One application may use information of an image not useful to another application. In biometrics, for example, a face image contains information not useful to a fingerprint machine expert. Ideally a qual-

ity model involves features, which are preferably related to each other, i.e. features which are reusable even for different applications. In this work symmetry features are used to automatically assess the quality of fingerprint images, but also an indication of their appliance in face images is given. We can not use more than general models when trying to estimate the quality of biometric images, since a high-quality reference image of the same individual is usually not available, i.e. the link to the individual may not be established in advance.

Once available, the benefits of having an automatic quality estimate include the following: First, when acquiring biometrics, all samples presented by a person (either for an enrolment or authentication purpose) can be checked automatically in terms of quality, this way enabling reasonable discrimination among individuals in the first place [3]. Second, in an authentication configuration involving several traits, e.g. face, fingerprint and speech, the quality of the presented images influences the weight given to the respective expert at fusion stage, where a final decision is made. The improvement of quality-aware fusion has been shown, although mainly involving quality assessment done by human experts [4, 5]. Thirdly, the the quality of an image might vary when considering only parts of it. For example, when measuring the similarity among biometric samples, high quality regions must be favoured [6, 7]. The three issues above are not only important in biometric recognition but also in other computer vision applications which involve visual recognition, e.g. object recognition, image database retrieval, etc.

As a result of recent fingerprint verification competitions involving particularly low quality impressions, even state-of-the-art algorithms’ performance decreases remarkably [8]. Recent advances in fingerprint quality assessment include [7, 3, 9]. The novelty of this study consists in the continuous modeling of all details in a fingerprint allowing them to be used for dual purposes, recognition and quality estimation. Additionally, while there are limited efforts devoted to the study of fingerprint image quality, to the best of our knowledge no studies have reported on face image

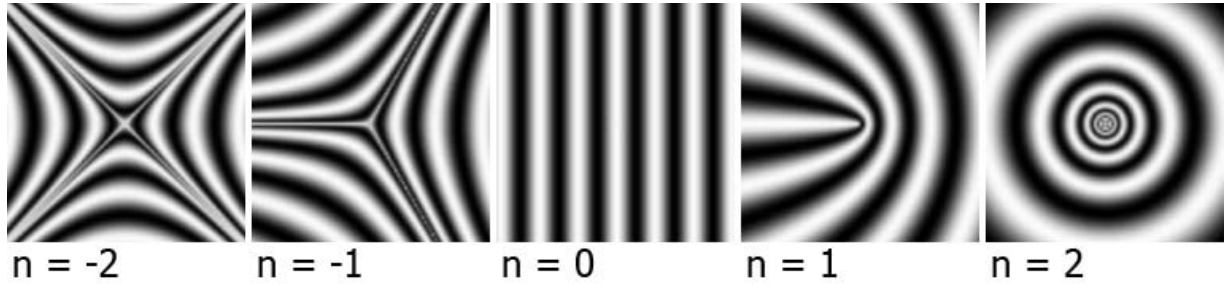


Figure 1. Patterns with orientation description  $z = \exp(in\phi)$

quality.

We will first describe our general approach to quality assessment, and give further details in the case of fingerprint and face images. We report quantitative and comparative experimental results involving a different fingerprint quality estimation method [3], as well as, manual (independent of this study) quality indices assigned to the fingerprints of the QMCYT database [5, 10]. Two fingerprint recognition systems [3, 6] are employed to study the effects of fingerprint quality on the two systems, and, to observe how well manually and automatically assigned quality indices are agreeing.

## 2. Quality Assessment Features

The orientation tensor holds edge information, which is exploited in this work to draw conclusions on the quality of an image. Our target is to determine whether the information is structured in some sense, i.e. to distinguish noisy content from possibly non-trivial structures. The latter are for example essential for recognition tasks, representing the individuality of a biometric sample. Our method principally decomposes the orientation tensor of an image into symmetry representations, where the included symmetries are related to the particular definition of quality. Whether or not a test image comprises these symmetries, will be a factor determining the quality metric. The orientation tensor is given by the equation

$$z = (D_x f + iD_y f)^2, \quad (1)$$

where  $D_x f$  and  $D_y f$  denote the partial derivatives of the image w.r.t. x- and y-axes. The squared complex notation directly encodes the double angle representation. For the computation of the derivatives, separable Gaussians with a small standard deviation are used. Next, the orientation tensor is decomposed into symmetry features of order  $n$ , where the  $n$ th symmetry is given by  $\exp(in\phi + \alpha)$  [11, 12, 14, 13]. The corresponding patterns are shown in figure 1, e.g. straight lines for  $n = 0$ , parabolic curves and line endings for  $n = \pm 1$ , circles, spirals and stars for  $n = \pm 2$ . In figure 1, the so called class member  $\alpha$  is zero.

Filters modeling these symmetry descriptions can be obtained by

$$h_n = (x + iy)^n \cdot g \quad \text{for } n \geq 0, \quad (2a)$$

$$h_n = (x - iy)^{|n|} \cdot g \quad \text{for } n < 0, \quad (2b)$$

where  $g$  denotes a 2D Gaussian with standard deviation ( $\sigma$ ). These features are invariant to position, rotation, and (locally) to scale. For a more detailed review of symmetry filters, i.e. symmetry derivatives of Gaussians, we refer to [13]. Decomposing an image into certain symmetries involves calculating  $\langle z, h_n \rangle$ , where  $\langle \cdot, \cdot \rangle$  denotes the 2D scalar product, yielding complex responses  $s_n = c \cdot \exp(i\alpha)$ , with  $c$  representing the certainty of occurrence and  $\alpha$  (class member) encoding the pattern orientation of symmetry  $n$  (for  $n \neq 2$ ). Normalized filter responses are obtained calculating  $\hat{s}_n = \frac{\langle z, h_n \rangle}{\langle |z|, h_0 \rangle}$ , by dividing  $s_n$  through the amount of certainty. In this way,  $\{\hat{s}_n\}$  describe the symmetry properties of an image in terms of  $n$  orders. The  $n$ s can be chosen to match the expected symmetries in a candidate image, thus modeling a reference image by a limited number of symmetry features. The definition of quality for a specific application determines the orders and scales ( $\sigma$ ) used by this model. Furthermore, we demand  $\{\hat{s}_n\}$  to be well separated over the image plane, in that we look for a high and dominant symmetry at each point. Equation 3 denotes a simple inhibition scheme [14]

$$\hat{s}_n^i = s_n \cdot \prod_k (1 - |\hat{s}_k|), \quad (3)$$

where  $k$  refers to the remaining applied orders, to sharpen the filter responses. Consequently, a high certainty of one symmetry type imposes a reduction of the other types. Second, we calculate the covariance among  $\{|\hat{s}_n^i|\}$  in blocks of size  $b \times b$ . It is assumed that a large negative covariance is desirable in terms of quality, because this suggests well separated symmetries with reliable certainty measures  $c$ . On the other hand, positive covariance implies the co-occurrence of mutually exclusive symmetry types in the vicinity of a point, which we consider an indication for noise or blur.

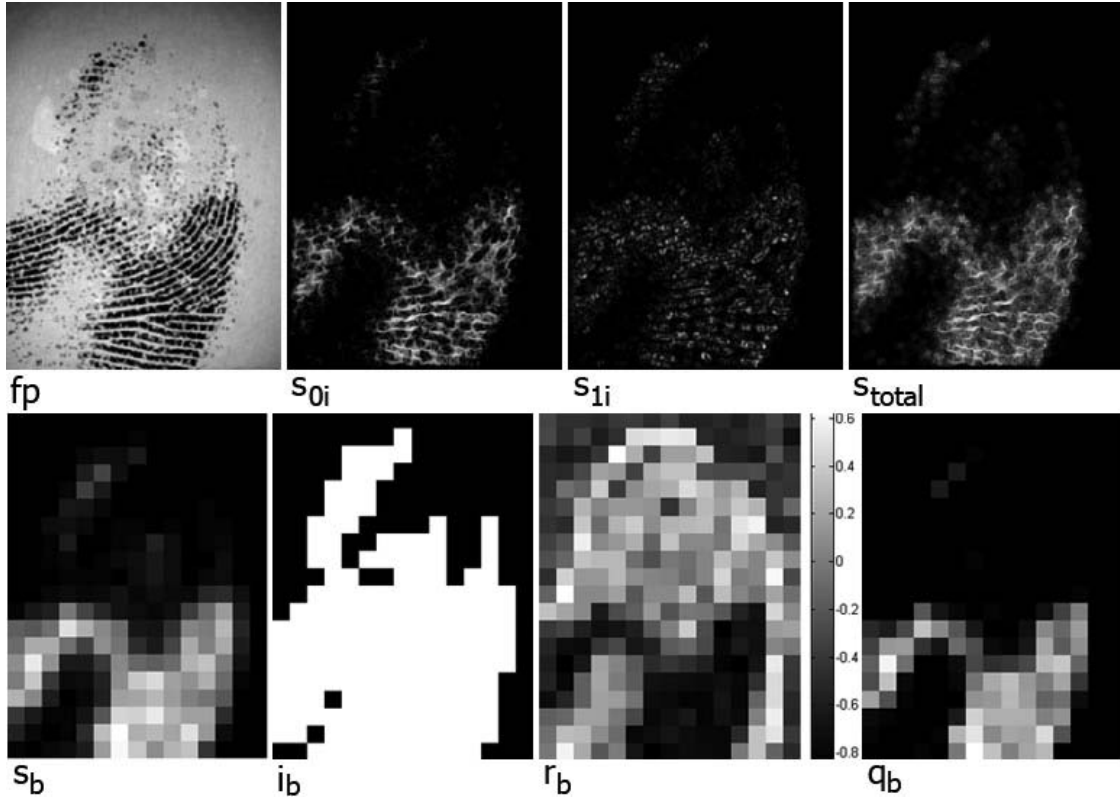


Figure 2. Top row: Decomposition of the example fingerprint into inhibited linear and parabolic symmetry ( $s_{0i}, s_{1i}$ ) and their combination ( $s_{total}$ ); Bottom row: Intermediate steps in fingerprint quality estimation, i.e. the blockwise average of the total symmetry ( $s_b$ ), the interesting blocks ( $i_b$ ), the blockwise correlation of the symmetries ( $r_b$ ), and the final weighted quality ( $q_b$ )

We incorporate this information by weighting the symmetry certainty. Simply summing  $\{\hat{s}_n^i\}$  at each pixel gives a total symmetry image  $s_{total}$ , which is further averaged in blocks of size  $b \times b$  yielding  $s_b$ . The quality measure  $q_b$  for each block is given by

$$q_b = y(|r_b|) \cdot \chi(-r_b) \cdot s_b, \quad (4)$$

where  $\chi$  represents the Heavyside function (1 for positive arguments, 0 otherwise) and  $r_b$  denotes the correlation coefficient among  $\{|\hat{s}_n^i|\}$  for block  $b$ . The quantity  $r_b$  is calculated as an average of the correlation coefficients between any two involved orders  $r_{b_{k,l}}$ , as defined by

$$r_{b_{k,l}} = \frac{\text{Cov}(|s_k^i|, |s_l^i|)}{\sqrt{\text{Var}(|s_k^i|)\text{Var}(|s_l^i|)}} \quad (5)$$

Note that  $r_{b_{k,l}} = r_{b_{l,k}}$ , and that in case of employing only two orders for the decomposition, e.g. 0 and 1,  $r_b$  simply is  $r_{b_{01}}$ . The expression  $\chi(-r_b)$  indicates a contribution of  $s_b \neq 0$  if and only if the corresponding  $r_b$  is negative. The mapping function  $y$  controls the influence of  $r_b$  and is

chosen empirically, e.g.  $y(t) = t^2$  makes the method very strict. A final quality metric is established by averaging  $q_b$  over the “interesting” blocks  $i_b$ , which are represented by blocks where  $s_b > \tau$ , thus having a minimum total symmetry response. The proposed technique is demonstrated in two applications, namely automatic fingerprint and face image quality estimation.

### 3. Applications

#### 3.1. Fingerprint quality assessment

By human experts, the quality of a fingerprint image is usually expressed in terms of the clarity of ridge and valley structures, as well as the extractability of certain points (minutiae, singular points) [7]. We can model the behaviour of the orientation tensor of a typical fingerprint entirely with symmetry features. On one hand, a coherent ridge flow has linear symmetry and thus can be modeled by symmetry features of order 0. On the other hand, minutiae points such as ridge bifurcation and ending have parabolic symmetry and can be modeled by symmetry features of order 1.

Other prominent points in fingerprints such as core and delta points can likewise be modeled by symmetry features of order 1 and -1 respectively. Intuitively, features of order  $|n| > 1$  are considered not meaningful here and are therefore omitted. Also, order 1 can represent both 1 and -1 since the filters respond similarly at singular points of different type, and no further classification is needed. This means that only three scalar products are needed with the orientation tensor,  $\langle z, h_0 \rangle$ ,  $\langle |z|, h_0 \rangle$  and  $\langle z, h_1 \rangle$ . The first two scalar products essentially correspond to averaging the orientation tensor  $z$  and its magnitude  $|z|$  respectively, whereas the last scalar product corresponds to a complex derivation of  $z$ . All convolutions can be implemented employing 1D Gaussian filters and their derivatives, e.g.  $\langle z, h_1 \rangle = \langle (x + iy) \cdot g, z \rangle = \langle x \cdot g(x) \cdot g(y), z \rangle - i \langle y \cdot g(y) \cdot g(x), z \rangle$ . By following the concepts above, we obtain two inhibited symmetry images  $s_0^i$  and  $s_1^i$  and a total symmetry image  $s_{total}$ .

The top row in figure 2 depicts these results for an example fingerprint of the FVC2004 database. As can be seen,  $s_{total}$  contains the relevant portion of the image.  $s_0^i$  and  $s_1^i$  are relatively well defined (the image is actually of bad quality) at linear and parabolic symmetry neighbourhoods respectively. Furthermore we divide the total symmetry into blocks  $s_b$  and identify interesting blocks  $i_b$ . Last we calculate the correlation coefficient  $r_b$  in blocks between  $s_0^i$  and  $s_1^i$ . The images containing these blocks for the example fingerprint are displayed at the bottom of figure 2. We observe, that the covariance is negative in reasonably good-quality regions, whereas it is positive in noisy and bad-quality regions. This separation is less apparent when considering  $s_b$  only. The bottom right image in figure 2 contains quality blocks  $q_b$ , which are a weighted version of  $s_b$  (compare equation 4). Looking at the latter, bright blocks indicate good quality. We average  $q_b$  over the number of interesting blocks in  $i_b$ , to obtain an overall quality metric  $Q$ . This metric lies in  $[0, Q_{max}]$  for some  $Q_{max} \leq 1$  depending on the choice of  $y$ . Although we have confined our reporting to boosting recognition rates, it should be noted that  $q_b$  can also be used in other fingerprint processing modules, e.g. to steer a fingerprint enhancement process and to make feature extraction or matching more robust.

The few published studies on fingerprint quality assessment methods measure spatial coherence of the ridge flow only, by essentially determining or approximating  $s_0$ . Additionally the latter is commonly partitioned into blocks ( $s_{0_{avg}}$ ), which are then weighted decreasingly with distance to the fingerprint's centroid when calculating a quality metric. Inspecting, figure 4 reveals that this strategy may not be enough, because important regions such as singular points (e.g. core, delta) and minutiae are per definition incoherent to the ridge flow, and their presence therefore automatically impairs the estimated quality. In figure 4, averaged  $s_0$  and our metric is shown on an image from the QMCYT

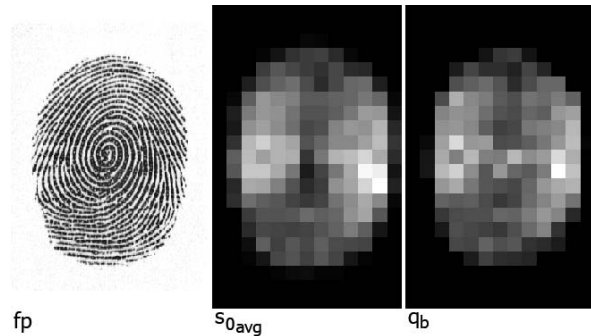


Figure 4. Illustrating the difference  $s_{0_{avg}}$  and  $q_b$ . Here we can see that the core point is misinterpreted in terms of quality when just averaging  $s_0$

database. Quantitative results with comparisons will be presented further below.

### 3.2. Face quality assessment

To show that the proposed method is not restricted to quality assessment of fingerprint images only, we demonstrate its usability for another biometric trait, i.e. to estimate the quality of face images. In terms of quality definition we can restate the demand for clarity of linear structures. In addition we can also expect circular patterns (e.g. eyes, nostrils) in a face image. For this reason we model the orientation tensor with symmetry features of orders 0 and 2 here. Depending on the size of the face in the image, ( $\sigma$ ) may be adjusted when decomposing the tensor. Except this, the same steps as detailed above are applied in order to determine the quality measure. When constructing  $s_2$ , we calculate  $\langle z, h_2 \rangle = \langle (x + iy)^2 \cdot g, z \rangle = \langle x^2 \cdot g(x) \cdot g(y), z \rangle - \langle y^2 \cdot g(y) \cdot g(x), z \rangle - i2 \langle x \cdot g(x) \cdot y \cdot g(y), z \rangle$ , involving separable Gaussians and their 1st and 2nd order derivatives. Thus, all convolutions are reduced to one dimension again. Furthermore, we apply a simple self damping of  $s_2$  in neighbourhoods where  $\arg(s_2) \neq 0$ , refining  $s_2 = s_2 \cdot |\cos(\arg(s_2))|$ , to focus on class member  $\alpha = 0$  (compare last pattern in figure 1).

The top row of figure 3 shows a (cropped) example image of the XM2VTS database, and the corresponding total symmetry image  $s_{total}$ . The latter contains the relevant portions of the image, as can be observed. Following the steps above,  $q_b$  is calculated along blocks, yielding the image displayed to the right of  $s_{total}$ . Here,  $q_b$  is bright, wherever  $s_{total}$  is defined ( $s_b > \tau$ ). In order to show the effects of noise on  $q_b$ , we degrade the example image by adding Gaussian noise. This is visualized in the second row of figure 3. The presence of heavy noise counteracts the dominance of a single symmetry at a point, and, in addition gives rise to multiple filter responses where no focused structure is present.



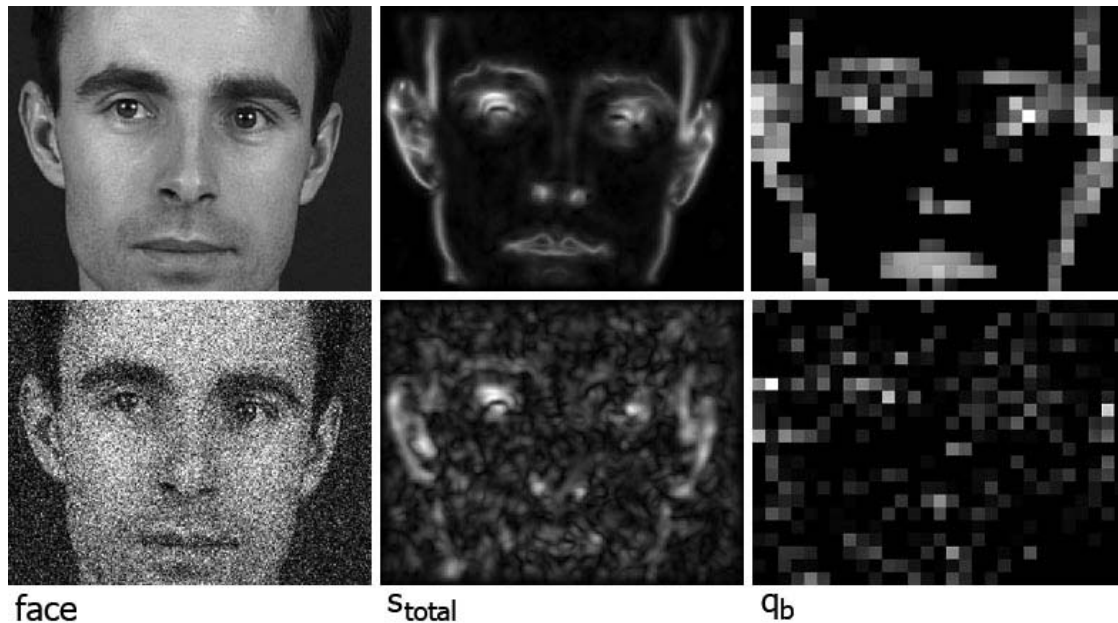


Figure 3. Quality assessment for two face images

This has an impact on the covariance between the different orders, which in turn decreases the combined certainty of the symmetries and thus the quality measure. In the example of figure 3, the estimated quality decreases by  $\approx 70\%$ .

A quantitative face image quality assessment is not possible to present, because a publicly available and independently annotated database is lacking.

#### 4. Experiments

We use a recently developed fingerprint recognition system [6] for the experiments. It applied some features out of the ones used for quality assessment above, but in a manner primarily targeting on measuring the similarity among fingerprints. The system efficiently worked with symmetry features of order 0 and 1 throughout the whole process of fingerprint alignment and matching. Only “well-defined” regions of two fingerprints were considered for comparison, which already indicated some quality awareness of the system. In what follows it is referred to as system A. All experiments are conducted on the QMCYT fingerprint database [10], defining 750 fingerprints \* 12 impressions. For each impression a manually annotated (independent of this study) quality label [15] was available. We compared these to the automatically determined ones. To further extend experimental possibilities we also use the publicly available NIST<sup>1</sup>FIS2 software for both fingerprint

<sup>1</sup>National Institute of Standards and Technology

recognition, termed system B here, and fingerprint quality assessment (NFIQ). It is worth mentioning that the grading by the proposed method is continuous in  $[0,1]$ , whereas it is discrete for NFIQ and the human expert being in  $[1..5]$  and  $[0..9]$  respectively. When applicable, the latter two output ranges are normalized into  $[0..1]$ .

First we show how the fingerprints are distributed in terms of quality according to the different quality assessment methods. Looking at figure 5, the estimated (proposed method) and empirical (human opinion) distributions show very promising similarities, whereas the proportioning by the second automatic estimator is deviating notably. Second we want to use these quality labels to show the connection between recognition performance and quality of the involved impressions, i.e. we want to examine the validity of the quality assessment. We can do this by partitioning the available fingerprints into “quality groups”, and test the recognition performance taking only samples within the same quality group. The 750 fingerprints are split into 5 equally sized partitions of increasing quality. The criteria for a fingerprint to be part of a certain group included the average quality of its impressions. For each group we perform 150x9 genuine and 150x74 imposter trials. We show the EER of the two recognition systems for all quality groups, where the partitioning of the fingerprints is based on the different quality assessment methods (see figure 6). Observe that recognition performance significantly increases along with image quality, in particular when considering only the two lowest quality groups. Also note that the proposed esti-

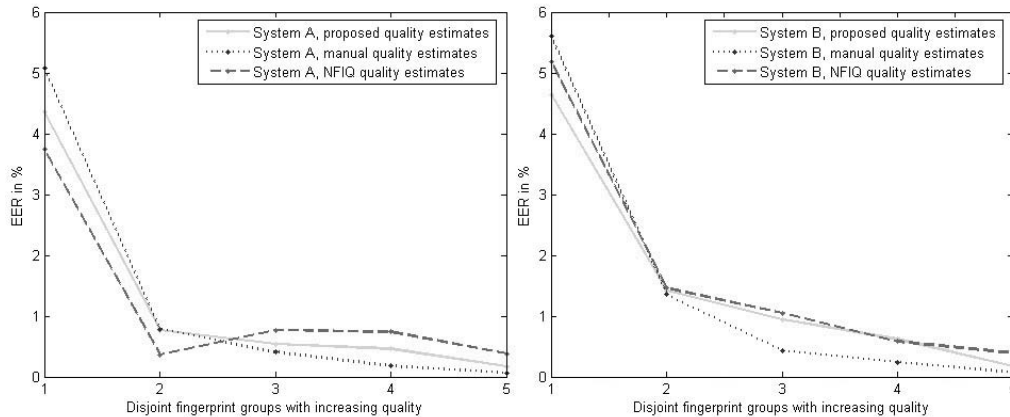


Figure 6. EER for system A and B on established quality groups: The latter are derived by means of the indicated quality assessment method

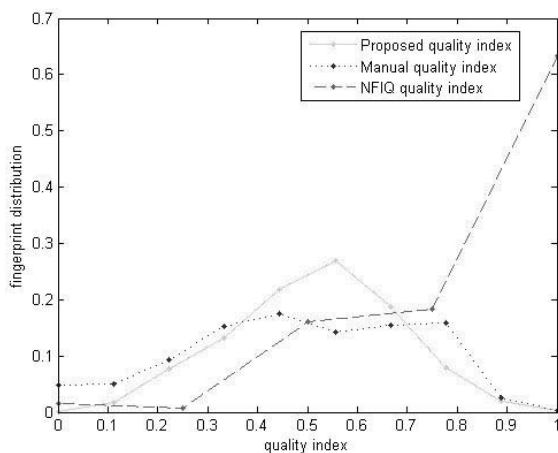


Figure 5. Fingerprint quality distributions (1 is the highest quality index)

mator comes closest to the human expert's quality grading.

## 5. Conclusion

In this work we proposed a reduced-reference image quality assessment method, and showed its interdisciplinary applicability in two biometric traits, face and fingerprint images. As the experimental results on fingerprint quality estimation underline, the proposed method compares well with a human experts opinion. The results are in significant favor of the novel quality measure in comparison with other quality metrics, NIST NFIQ. To the best of our knowledge, this level of agreement with human opinion has not been reported before. The two test fingerprint verification systems show a monotonically increasing performance when only fingerprints given continuously higher and higher quality by

our estimator are involved. This leads to an EER of 0.2% which is significantly better than using no-quality metrics. Future work includes the study of using linear combinations of symmetries of different orders to model the tensor, instead of pushing one dominant symmetry. Furthermore, we plan to experiment with different kinds of image degradations, particularly for the face image case.

## References

- [1] Wang, Z., Bovik, A., Sheikh, H., Simoncelli, E.: Image Quality Assessment: From Error Visibility to Structural Similarity. *IEEE Trans. Image Processing* **13** (2004) 1
- [2] Eskicioglu, A.M., Fisher, P.S.: Image quality measures and their performance. *IEEE Trans. Communications* **43** (1995) 2959–2965 1
- [3] Tabassi, E., Wilson, C., Watson, C.: Fingerprint Image Quality. Technical Report NISTIR7151, Nist (2004) 1, 2
- [4] Bigun, J., Fierrez-Aguilar, J., Ortega-Garcia, J., Gonzalez-Rodriguez, J.: Multimodal biometric authentication using quality signals in mobile communications. In: Proc. of 12'th Int. conf. on image analysis and processing, Mantova, Italy, IEEE Computer Society Press, Piscataway, NJ (2003) 2–11 1
- [5] Fierrez-Aguilar, J., Munoz-Serrano, L.M., Alonso-Fernandez, F., Ortega-Garcia, J.: On the effects of image quality degradation on minutiae- and ridge-based automatic fingerprint recognition. In: IEEE Intl. Carnahan Conf. on Security Technology ICCST, Las Palmas de Gran Canaria, Spain, IEEE Press (2005) 1, 2
- [6] Fronthaler, H., Kollreider, K., Bigun, J.: Local Feature Extraction in Fingerprints by Complex Filtering. In: International Workshop on Biometric Recognition Systems IWBR 2005, Beijing, China. Volume 3781., Springer (2005) 77–84 1, 2, 5

- [7] Chen, Y., Dass, S., Jain, A.: Fingerprint Quality Indices for Predicting Authentication Performance. In: Audio- and Video-based Biometric Person Authentication (AVBPA) 2005, Rye Brook, New York. (2005) 160–170 [1](#), [3](#)
- [8] Maio, D., Maltoni, D., Cappelli, R., Wayman, J., Jain, A.: FVC2004: Third Fingerprint Verification Competition. In: International Conference on Biometric Authentication (ICBA04), Hong Kong. (2004) 1–7 [1](#)
- [9] Lim, E., Jiang, X., Yau, W.: Fingerprint quality and validity analysis. In: IEEE International Conference on Image Processing. Volume 1., IEEE (2002) 469–472 [1](#)
- [10] Ortega-Garcia, J., Fierrez-Aguilar, J., Simon, D., Gonzalez, J., Faundez-Zanuy, M., Espinosa, V., Satue, A., Hernaez, I., J.-J.Igarza, Vivaracho, C., Escudero, D., Moro, Q.I.: MCYT baseline corpus: A bimodal biometric database. IEE Proc. VISIP **150** (2003) 395–401 [2](#), [5](#)
- [11] Bigun, J.: Recognition of Local Symmetries in Gray Value Images by Harmonic Functions. In: Ninth International Conference on Pattern Recognition, Rome, IEEE Computer Society Press (1988) 345–347 [2](#)
- [12] Knutsson, H., Hedlund, M., Granlund, G.H.: Apparatus for Determining the Degree of Consistency of a Feature in a Region of an Image that is Divided into Discrete Picture Elements. In: US. patent, 4.747.152. (1988) [2](#)
- [13] Bigun, J., Bigun, T., Nilsson, K.: Recognition by symmetry derivatives and the generalized structure tensor. IEEE-PAMI **26** (2004) 1590–1605 [2](#)
- [14] Johansson, B.: Low Level Operations and Learning in Computer Vision. PhD thesis, Linköping University, Sweden, Linköping University SE-581 83 Linköping, Sweden (2004) Dissertation No. 912, ISBN 91-85295-93-0. [2](#)
- [15] Simon-Zorita, D., Ortega-Garcia, J., Fierrez-Aguilar, J., Gonzalez-Rodriguez, J.: Image quality and position variability assessment in minutiae-based fingerprint verification. IEE Proceedings Vision, Image and Signal Processing, Special Issue on Biometrics on the Internet **150** (2003) 402–408 [5](#)